

Understanding and Co-designing the Data Ingestion Pipeline for Industry-Scale RecSys Training

Mark Zhao*
Stanford University
Stanford, USA

Bugra Gedik
Facebook
Menlo Park, USA

Rakesh Komuravelli
Facebook
Menlo Park, USA

Haowei Lu
Facebook
Menlo Park, USA

Kevin Wilfong
Facebook
Menlo Park, USA

Christos Kozyrakis
Stanford University
Stanford, USA

Niket Agarwal
Facebook
Menlo Park, USA

Satadru Pan
Facebook
Menlo Park, USA

Jerry Pan
Facebook
Menlo Park, USA

Sundaram Narayanan
Facebook
Menlo Park, USA

Harsha Rastogi
Facebook
Menlo Park, USA

Parik Pol
Facebook
Menlo Park, USA

Aarti Basant
Facebook
Menlo Park, USA

Mustafa Ozdal
Facebook
Menlo Park, USA

Tianshu Bao
Facebook
Menlo Park, USA

Jack Langman
Facebook
Menlo Park, USA

Carole-Jean Wu
Facebook
Menlo Park, USA

Abstract

The data ingestion pipeline, responsible for storing and pre-processing training data, is an important component of any machine learning training job. At Facebook, we use recommendation models extensively across our services. The data ingestion requirements to train these models are substantial.

In this paper, we present an extensive characterization of the data ingestion challenges for industry-scale recommendation model training. First, dataset storage requirements are massive and variable; exceeding local storage capacities. Secondly, reading and preprocessing data is computationally expensive, requiring substantially more compute, memory, and network resources than are available on trainers themselves. These demands result in drastically reduced training throughput, and thus wasted GPU resources, when current on-trainer preprocessing solutions are used.

To address these challenges, we present a disaggregated data ingestion pipeline. It includes a central data warehouse built on distributed storage nodes. We introduce Data PreProcessing Service (DPP), a fully disaggregated preprocessing service that scales to hundreds of nodes, eliminating data stalls that can reduce training throughput by 56%. We implement important optimizations across storage and DPP, increasing storage and preprocessing throughput by 1.9×

and 2.3×, respectively, addressing the substantial power requirements of data ingestion. We close with lessons learned and cover the important remaining challenges and opportunities surrounding data ingestion at scale.

1 Introduction

Massive amounts of training data is fueling the industry-wide paradigm shift towards applications centered around machine learning (ML), and especially deep learning, models [26, 42]. Training these models requires a *data ingestion pipeline*, consisting of a slew of supporting storage, reading, and preprocessing services that feed trainers with data. However, compared to model training itself, the data ingestion pipeline has received little consideration. For large scale training, understanding and scaling data ingestion pipelines is essential, as inefficiencies can cripple training throughput [36]. Increasingly complex models and faster ML accelerators such as GPUs [13] and TPUs [23] are massively increasing training throughput demands at a per-chip and system scale [4], further galvanizing the need for a scalable and efficient data ingestion solution.

At Facebook, our scale presents a host of complex and novel challenges for ML data ingestion. While recent work has explored various isolated components of the data ingestion pipeline such as preprocessing [38], filesystems [53], reading [24, 52], or caching [29, 36], there is still relatively

*Work done while at Facebook.

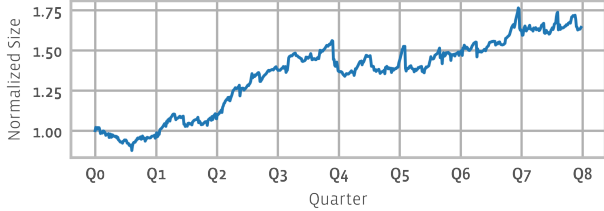


Figure 1. Normalized training dataset size across our recommendation models. Physical bytes are in the exascale and have grown by 75% in the past two years.

little understanding of the end-to-end challenges and requirements in industry-scale environments like ours. This paper presents an in-depth analysis of ML data ingestion requirements at scale, and how we architect and optimize our end-to-end data ingestion pipeline for these requirements.

We focus on deep learning personalized recommendation systems (RecSys). We do so for two reasons. First, they enable important components and services across a wide breadth of domains, seeing widespread adoption at Facebook [8, 19–21, 34], Google [12, 15, 23], Microsoft [18], Baidu [50], and many other hyperscale companies [41, 51]. Secondly, training these models, which often consist of trillions of parameters [32, 37], places enormous demands on the end-to-end training and data ingestion pipeline. Training a production recommendation system takes weeks, requiring numerous training jobs each using hundreds of distributed GPUs.

We begin by quantifying challenges these training jobs present to the data ingestion pipeline. Our datasets are massive, requiring tens of petabytes of storage per model and exabytes cumulatively, and are constantly growing and changing. Figure 1 highlights how our training datasets for recommendation models have grown by around 75% in the past two years. In addition to storage, feeding hundreds of distributed GPUs requires highly resource-intensive preprocessing operations. We demonstrate that current on-trainer preprocessing solutions are heavily constrained on network, memory, and compute resources. This results in data stalls that can cut trainer throughput in half, wasting valuable GPU resources. Furthermore, we show that there is no one size fits all solution; storage and preprocessing requirements vary heavily across models and training jobs.

Informed by our system requirements, we present the end-to-end data ingestion pipeline at Facebook. It consists of disaggregated storage, preprocessing, and training nodes which can be scaled-out and right-sized to meet the diverse needs of our ML models. We describe how we store training data in structured data warehouses built on top of a distributed filesystem. We also present *Data PreProcessing Service (DPP)* that performs preprocessing operations using disaggregated compute nodes, scaling to eliminate data stalls



Figure 2. Percent of storage, preprocessing, and training power required to train three production recommendation models. 50% line emphasizes data ingestion can require more power than training.

while supplying training data to distributed trainers. Depending on model and trainer requirements, DPP can scale from 10s to 100s of preprocessing nodes for a single training job.

Next, we present efficiency optimizations co-designed across storage and DPP. These optimizations are important, as Figure 2 shows how *storage and preprocessing can consume more power than the actual GPU trainers themselves!* Since power is the limiting resource in our datacenters [10], improving data ingestion efficiencies can directly augment our training capacity. We demonstrate how feature flattening, in-memory flatmaps, feature regrouping, and merged reads help reduce the data ingestion power consumption by 2.2×.

Specifically, we make the following contributions:

- We perform a first-principles characterization of the end-to-end training data ingestion requirements, focusing on industry-scale recommendation models.
- We present an end-to-end data ingestion architecture that is optimized and scalable.
- We discuss lessons learned in architecting DPP and research challenges and new opportunities in the area of large scale training data ingestion.

2 Background

In this section, we provide an overview of our recommendation models and data ingestion pipelines. We describe unique characteristics of training recommendation models at scale and how they impact the data ingestion pipeline.

2.1 Recommendation Models

Personalized recommendation models are used to suggest new content to users based on their past preferences. These models are highly potent across a breadth of tasks. They leverage features from the user and the set of potential recommendations, and output a prediction of how likely the user is to interact with each possible recommendation (e.g., click-through rate). For example, video hosting sites may recommend new videos to a user based on the duration and genre of videos he or she has previously watched. An online shopping platform may recommend a product based on its ratings, as well as products a user has purchased previously.

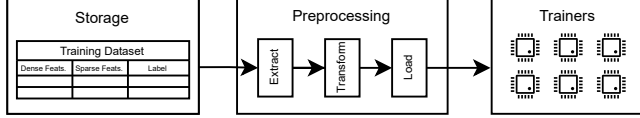


Figure 3. Functional view of the data ingestion pipeline. Throughput demands are driven by the trainers.

We train recommendation models through a process called mini-batch stochastic gradient descent (SGD) [44], similar to most vision and natural language processing (NLP) models. SGD generalizes a model to complex distributions by iteratively updating the model’s weights to minimize a loss function, given successive *mini-batches* of preprocessed training examples. Each training example is represented as a preprocessed tensor of *features*, along with a label.

To improve training throughput, we leverage data [28] and model [16] parallelism by replicating and sharding the model across multiple trainers. We concurrently distribute different mini-batches to each trainer. Trainer nodes synchronize embeddings, activations, and gradients with each other using collective communication primitives. This process iterates until a certain metric is reached (e.g., validation accuracy, change in validation loss, etc.).

2.2 Data Ingestion Pipeline

Figure 3 shows a functional overview of the end-to-end training workflow. The data ingestion pipeline is responsible for both *storing* the training dataset and *preprocessing* raw bytes into tensors ready for training.

Storing Training Data. Training datasets for recommendation models are represented as structured rows in tabular format, each containing features and labels. Features represent the vast majority of stored bytes (> 99%). Each training sample is associated with two types of features: dense and sparse. Each dense feature represents a continuous value, such as user age or current time, and is stored as a floating point number. Each sparse feature consists of a *variable length* list of categorical values, such as the IDs of pages a given user likes, stored as integers. Some sparse features optionally associate each categorical value with a floating point "score", which may be used to weigh categorical values based on metadata (e.g., page creation time).

Training samples are generated from event logs via an offline preprocessing step not on the critical path of training. Thus, each sample will not only contain a large number of both sparse and dense features, but the exact features present in each sample can vary. For example, device or browser specific features may only be generated depending on how a user accesses our services. Each feature is directly mapped to a unique feature ID, and the percent of samples containing a feature is denoted as its *coverage*. The length of each sparse feature also varies based on the original event log.

Preprocessing. Preprocessing is the job of transforming raw bytes in storage into *materialized* tensors in trainer memory, ready for use during SGD. Preprocessing is commonly subdivided into three phases: extract, transform, and load.

Raw bytes are *extracted* from storage and decoded into individual training samples. Depending on how and where the data is stored, this process may involve decryption, decompression, reconstruction, and other format transformations in order to obtain the training sample (i.e., table row). Furthermore, each recommendation model sample typically contains more features than are required by a given model; unused features must be filtered out.

Training samples are next *transformed* into a format ingestible by trainers. Float values may be normalized, and categorical values may be hashed, clipped, or even sorted. New features may even be derived from multiple raw features, adding significant compute complexity. For example, by using sparse features representing users’ favorite pages and a classification of each page, we can derive a feature representing their categories of interest (e.g., movies, musicians, authors, etc.) on-the-fly. Each training job can specify unique feature sets and transformation configurations; offline pre-computation and storing all possible transformations and combinations of derived features is intractable.

Once features are preprocessed, they are batched together into materialized tensors. These are *loaded* into trainers themselves, usually by placing them in device memory (e.g., the HBM of GPUs). Preprocessing is on the critical path of training, and typically runs concurrently in a pipelined manner until training is complete.

2.3 Industry-Scale RecSys Training

Training recommendation models at our scale presents many unique challenges and requirements.

At Facebook, we use hundreds of distinct recommendation models in production across our services, each developed and updated continuously via a host of individual training jobs. These models are collaboratively trained by hundreds of ML engineers, whose productivity is an essential resource. *Developers must be able to quickly access the necessary training datasets and author feature and preprocessing configurations across diverse model architectures.*

Furthermore, our most important and complex models are supported by tens to hundreds of engineers. To avoid conflicts, these are trained in a regimented model release process, which occurs over three phases. First, ML engineers *explore* their ideas (e.g., new features or architectural improvements) on top of the current production model through hundreds to thousands of small training jobs. Exploratory jobs generally require less compute and use a small fraction (e.g., < 5%) of its respective table’s total samples. Next, the most promising ideas are *combined* in various permutations to generate a small number of training jobs, on the order of tens to hundreds. These combo jobs are large and launched together,

demanding immense parallelism and the majority of the table. It is essential that the data ingestion pipeline can handle the high throughput demands placed by these concurrent jobs, as this phase is on the critical path for model release. Finally, the most promising *release candidates* are re-trained on fresh data, and the best model is deployed in production. While these jobs are large, there are relatively few of them.

This diversity in training job storage and throughput requirements is only compounded by the variability across model types, as we explore in Section 3. Thus, *developers must be able to quickly scale data ingestion resources to meet disparate requirements*.

Finally, recommendation models exhibit numerous differences in data ingestion compared to common vision and NLP, or content understanding (CU), models. Datasets are stored as structured rows in massive tables, as opposed to individual, unstructured files. As we show in Section 3.1, these datasets are massive and constantly changing to allow models to be trained to higher accuracy on fresh data.

However, an individual training job cannot hope to train on the entire dataset. Training jobs only require a portion of the dataset, specified by a certain number of timestamp partitions and specific features within each sample, over one epoch. Furthermore, feature sets and preprocessing configurations frequently differ between training jobs, even for one model. These characteristics result in limited data reuse opportunities. This is in stark contrast to common benchmark models and datasets which systematically ingest the entire dataset across multiple epochs, and systems that optimize for these characteristics [24, 29, 36, 47].

3 Understanding Data Ingestion Requirements at Scale

The data ingestion pipeline consists of multiple complex systems interacting at scale. We now seek to characterize and understand requirements that these systems must collectively satisfy. We focus on three representative recommendation models, denoted $RM_{1,2,3}$, that exhibit some of the highest resource demands and largest impact across our services.

3.1 Storage Requirements

As discussed in Section 2, our training datasets are stored in tables, partitioned by timestamps, that are constantly updated. Each job specifies a variable number of timestamp partitions to read; these cumulatively form the job’s dataset. Table 1 shows (compressed) size characteristics of each model’s respective training data table. It also shows the size of each timestamp partition in the table and the cumulative size of the timestamp partitions used by a representative release candidate training job for each RM . Training jobs use petabytes of data, which is significantly larger than the local storage capacity at each trainer node.

| Model | All Partitions (PB) | Each Partition (PB) | Used Partitions (PB) |
|-------|---------------------|---------------------|----------------------|
| RM1 | 13.45 | 0.15 | 11.95 |
| RM2 | 29.18 | 0.32 | 25.94 |
| RM3 | 2.93 | 0.07 | 1.95 |

Table 1. Compressed sizes of all table partitions, each partition, and the cumulative partitions used by a representative release candidate training job for each RM .

| % of Time Stalled | % CPU Utilization | % Memory BW Utilization |
|-------------------|-------------------|-------------------------|
| 56 | 92 | 54 |

Table 2. Stalls introduced by preprocessing on trainer hosts.

Furthermore, models are trained on shared compute infrastructure, using shared datasets. Even if every dataset could fit in local storage, duplicating it to each trainer node would be on the critical path of training and be highly inefficient. Similarly, even though individual training jobs only require a portion of stored timestamp partitions, we cannot discard unused data or store fully materialized tensors. Different models (and even analytics jobs) may reference the same table, and training jobs for a specific model may experiment across preprocessing configurations and feature sets.

Finally, as shown in Figure 1, our dataset sizes are continuously growing. This growth is driven by multiple factors, including organic user growth, reduced downsampling, and an increase in engineered features. These factors all imply that *we must serve training data from distributed storage*.

3.2 Throughput Demands

Bandwidth requirements of the data ingestion pipeline are driven by the distributed trainers. Data stalls are introduced when the throughput of any pipeline stage preceding the trainers is less than the aggregate throughput of the trainers themselves [36]. In such an event, GPUs will idle during each mini-batch iteration until sufficient data is provided, resulting in underutilization. This not only wastes accelerator resources, but also hinders engineers’ abilities to experiment and launch new models, directly impairing business metrics.

We first show that *current preprocessing solutions, which perform preprocessing on each training nodes’ CPUs, are insufficient*. To demonstrate this, we ran a training job for RM_1 on a training node, consisting of two 28-core x86 CPU sockets, two 100 Gbps NICs, and a total of 8 NVidia V100 GPUs. The trainer read from distributed storage, preprocessed each mini-batch using our production PyTorch [40] software stack, and performed training on the same machine. Table 2 shows that 56% of GPU cycles were spent stalled waiting for training data. The high CPU utilization shows that the trainer’s CPUs cannot preprocess data fast enough to serve the GPUs.

We next seek to understand the preprocessing bottlenecks in detail. To do so, we analyzed the preprocessing throughput

| | RM1 | RM2 | RM3 |
|------------------------|-------|------|-------|
| Node Throughput (GB/s) | 16.50 | 4.69 | 12.00 |

Table 3. Per-node trainer throughput requirements for RMs.

demanded by GPUs across RMs and traced through data extraction, transformation, and loading requirements.

3.2.1 GPU Trainers. First, we measured the preprocessing throughput required by each *RM*. We ran a production training job for each *RM* on a training node. We ensured that each GPU was not stalled on the data ingestion pipeline by serving materialized tensors from a large in-memory buffer.

Table 3 shows the corresponding per-trainer node GPU throughput requirements (i.e., the rate at which GPUs ingested materialized tensors) for each representative recommendation model. The results demonstrate that *GPU throughput requirements are not only significant, but vary by over 6× across models*. The difference in throughput across models is due to the variations in operational intensity (i.e., compute per sample) across models, as well as synchronization overheads between GPUs during each iteration.

This has multiple implications for the data ingestion pipeline. First, we project preprocessing throughput requirements to increase around 2 to 3.5× within the next two years due to larger training samples, improved hardware accelerators, and software optimizations. Secondly, we cannot simply over-provision resources for the worst-case model; doing so would waste large amounts of capacity and power across our fleet. The data ingestion pipeline must scale to meet intense and increasing GPU throughput demands, and adapt to the diverse requirements across models.

3.2.2 Data Loading. Section 3.1 established that we must load training data from distributed storage. This is done at each trainers’ host CPU, running a PyTorch runtime. We now show that *data loading over the network, even without extraction or transformation operations, requires a significant fraction of trainer CPU, network, and memory bandwidth*.

To understand the bare-minimum trainer front-end preprocessing resource requirements, we ran a dummy model on the same 2-socket, 8-GPU training node. The dummy model runs a full PyTorch runtime and training workflow, but simply drops tensors before sending them to the GPUs. This allowed us to measure the front-end resource utilization at given throughput requirements representative of each model. We created a service that provides fully materialized tensors, which the trainer runtime requests via an RPC call. We artificially limited the rate at which materialized tensors were fed into the trainer, and swept throughput until the two NICs saturated (which we measured to be at 20 GB/s).

Figure 4 shows the memory bandwidth and CPU utilization as ingestion rate increases. Vertical lines represent the

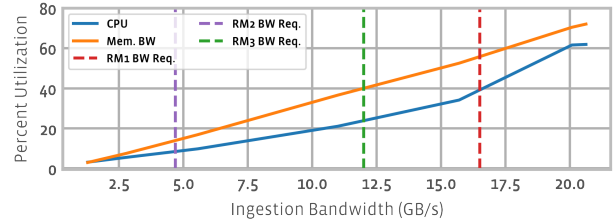


Figure 4. CPU and memory bandwidth utilization at trainer front-end as ingestion throughput scales using a dummy trainer.

| Model | kQPS | Storage RX (GB/s) | Transform RX (GB/s) | Transform TX (GB/s) | # Nodes Req. |
|-------|--------|-------------------|---------------------|---------------------|--------------|
| RM1 | 11.623 | 0.8 | 1.37 | 0.68 | 24.16 |
| RM2 | 7.995 | 1.2 | 0.96 | 0.50 | 9.44 |
| RM3 | 36.921 | 0.8 | 1.01 | 0.22 | 55.22 |

Table 4. Preprocessing worker throughput at saturation across RMs and # nodes required to meet trainer demands from Table 3. Storage traffic is compressed and transform output is uncompressed.

required GPU throughput across each *RM*, as measured in Table 3. We observe that CPU and memory bandwidth roughly linearly correlate with ingestion rate (until near saturation).

These results highlight how the high training data throughput demands driven by the GPUs directly translate to considerable front-end resource requirements for data loading. First, we observe that our models are approaching NIC saturation, even with significant reduction in data size due to preprocessing (see Section 3.2.3). Secondly, even without computationally expensive extraction or transformation operations, our models require up to 40% of CPU cycles (almost a full socket) and 55% of memory bandwidth. Digging deeper, we determined the largest contributors to CPU utilization were TLS decryption (38%), Thrift deserialization and user-space memory management (18%), and the Linux network stack (17%). Many of these operations represent a necessary “datacenter tax” when operating at industry scale [25]. Considering memory bandwidth approaches saturation at around 70% utilization, we are also approaching memory bandwidth limits. Scarce CPU and memory bandwidth resources are left for extracting and transforming training data.

3.2.3 Extracting & Transforming Data. While data loading is resource intensive, *data extraction and transformation require strikingly more resources than are available on trainers*.

To understand data extraction and transformation requirements, we ran the data extraction and transformation workload for each *RM* on a set of general-purpose servers with one 18-core x86 socket, 64 GB of memory, and 12.5 Gbps of networking. We used dedicated “worker” servers because it allows us to isolate data extraction and transformation costs, and it is representative of our current data ingestion pipeline infrastructure. We ran training on a separate training node

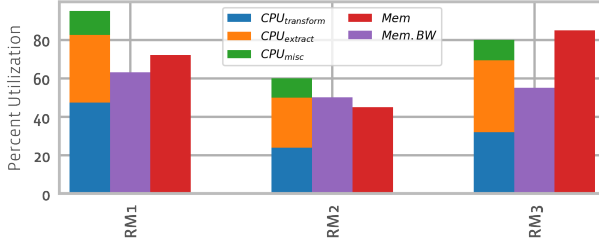


Figure 5. CPU, memory, and memory bandwidth utilization at preprocessing workers across RMs. CPU utilization is broken down into transformation, extraction, and miscellaneous cycles.

that requested materialized tensors via RPC calls, and we increased the request rate until each worker server saturated.

Table 4 shows the maximum data extraction and transformation throughput achieved by each preprocessing server. Based on these results, we need between 9 and 55 servers per trainer node to meet the GPU throughput demands in Table 3. This represents considerably more network, compute, and memory bandwidth resources than are available on trainers, especially when factoring in data loading requirements. Not only do models require a wide breadth of resources, each model’s requirements do not directly scale with GPU throughput requirements, *emphasizing the need to right-size preprocessing resources for each model’s characteristics*.

To understand the implications of these results in more detail, we first observe that preprocessing significantly reduces data size, especially considering storage bytes are compressed in Table 4. As we study in Section 4.2, this is due to a combination of filtering, over reading from storage, and size reduction during transformations. This has implications on network throughput requirements, as 1.18 to 3.64× more network bandwidth is required to extract raw samples from storage than to load materialized tensors. Thus, performing data extraction at the trainers would further amplify the network bandwidth requirements beyond the per-model requirements shown in Figure 4, resulting in data ingestion bottlenecks. Data extraction and filtering must be distributed.

Furthermore, network bandwidth is not the only limiting factor. Figure 5 shows CPU and memory bandwidth utilization at saturation. Each model exhibits diverse resource requirements. In fact, only RM_2 is bound on ingress NIC bandwidth as shown in Table 4.

RM_1 is bottlenecked on memory bandwidth and CPU utilization. As shown in Figure 5, this is because RM_1 requires significantly more CPU cycles for preprocessing due to its computationally expensive transformations. RM_3 is bound on memory capacity, forcing us to limit the worker thread pool size to avoid OOM exceptions. There is no one resource that we can easily provision on trainers to ensure that the data ingestion pipeline does not stall.

3.2.4 Summary. Section 3.1 demonstrated that we cannot store datasets in local storage in the trainers. Our throughput experiments showed that running preprocessing on each GPU training node is insufficient, as it requires a large and variable amount of resources. Over-provisioning storage, networking, and compute resources at training nodes to avoid data stalls is not reasonable. *We must disaggregate storage and preprocessing from training, and independently scale each out to meet data ingestion requirements.*

4 A Disaggregated and Co-designed Data Ingestion Pipeline

We now present the data ingestion framework at Facebook that enables us to efficiently meet the demanding and diverse data ingestion requirements from Section 3. Section 5 details how we implemented it within our datacenter ecosystem.

4.1 Disaggregated Architecture

Disaggregation is integrated across our data ingestion pipeline, as shown in Figure 6. It consists of three separate components: storage, DPP, and trainers; each is fully disaggregated. By disaggregating training storage, we have scaled our datasets to petabytes, enabled them to be constantly updated with fresh data, and centralized datasets to provide instant access across models and even analytics workloads. By disaggregating preprocessing with DPP, we can scale each training job to meet preprocessing throughput requirements, completely eliminating data stalls across our models. As we will describe in Section 4.3, disaggregating DPP is also central to ensuring preprocessing fault tolerance. By disaggregating trainers, we can train larger recommendation models and scale training throughput to meet distinct requirements of jobs across our model release process.

4.1.1 Distributed Storage. Figure 6 shows how we disaggregate storage by storing our datasets in a data warehouse on top of an exabyte-scale distributed filesystem. Each training sample is represented as a row, containing dense and sparse features, stored in partitioned Hive [46] tables. Dense features are typically stored in one column as a map between the feature ID and corresponding float value. Sparse features are typically subdivided into two columns. An ID List column maps each feature ID to a list of categorical values, while an ID Score List column also associates each categorical value with a floating point “score”.

Each table is encoded in a columnar file format, similar to Apache ORC [2]. Each feature column is then independently written to a separate *stream*. Streams are stored as files in Tectonic [39], Facebook’s exabyte-scale distributed filesystem. Tectonic subsequently splits files into filesystem blocks, which are Reed-Solomon [43] encoded into chunks, stored across Tectonic storage node disks.

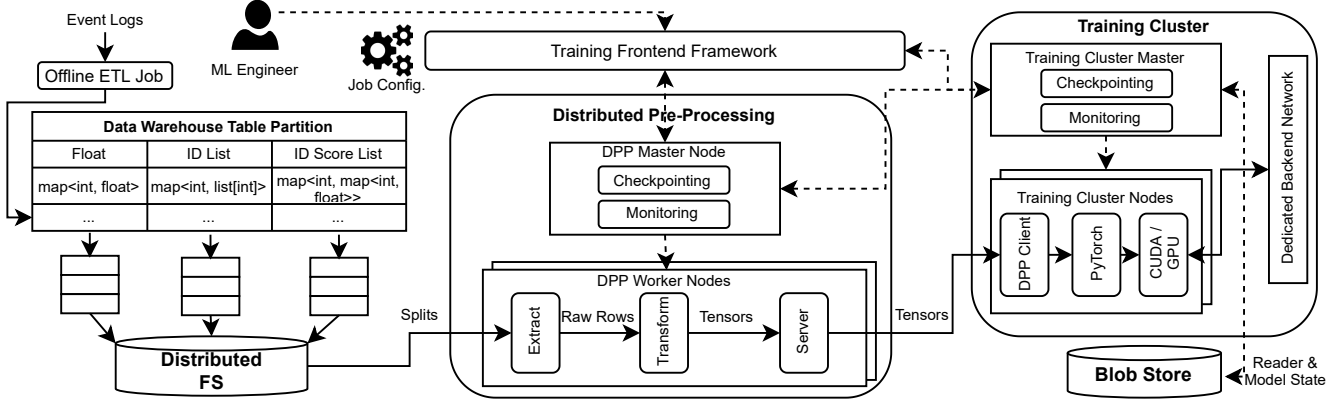


Figure 6. Our disaggregated data ingestion pipeline architecture. Solid and dashed lines represent data and control flow, respectively.

4.1.2 Scalable Preprocessing with DPP. DPP is central to our disaggregated data ingestion architecture. DPP is responsible for reading raw training data from storage, preprocessing it into ready-to-load tensors, and supplying the tensors to each training node’s PyTorch [40] runtime. We designed DPP to both scale to right-size resources and eliminate data stalls across disparate jobs, as well as enable vital productivity mechanisms for developers and ML engineers. We meet these requirements by dividing DPP into a data and control plane, which are independently designed to enable application throughput and ease-of-use, respectively. The control plane consists of a Master, and the data plane consists of DPP Workers and Clients.

DPP Control Plane. The DPP Master enables scalable work distribution by breaking down the entire preprocessing workload, across petabytes of data, into independent and self-contained work items for the data plane. It does so by exposing a simple *createSession(sessionSpec)* API. *createSession* accepts a DPP session specification that reflects the preprocessing workload, containing all of the required information to generate materialized tensors for each trainer. This includes the dataset table, specific partitions, required features, and preprocessing configurations for each feature.

From the table and partition information, the DPP Master will divide up the workload into a set of *splits*, each corresponding successive rows of the entire dataset. The Master maintains a global pool of splits, which it will serve as DPP Workers request work items, and tracks progress as work items are completed. In doing so, it can distribute work across hundreds of DPP Workers, as well as implement higher-order operations such as shuffling.

DPP Data Plane. DPP Workers and Clients are responsible for data plane operations of DPP.

Workers are designed to effortlessly scale out to eliminate data stalls. Workers are stateless, precluding any limit to how many Workers can exist in a given DPP session. They only communicate with the DPP Master (to fetch work items) and a limited number of DPP Clients (to serve tensors). On

startup, each Worker pulls a set of transformations from the Master, represented by a serialized and compiled PyTorch module, that it will use during preprocessing. Workers then continuously query for and execute work items from the DPP Master.

As shown in Figure 6, each work item requires Workers to extract, transform, and (partially) load training data. Specifically, Workers begin by reading, decompressing, and decrypting raw Tectonic chunks. Sets of raw chunks are then reconstructed into streams and decoded into raw table rows, filtering out unused features if necessary. Next, it applies the specified transformations to each raw feature using custom-built C++ binaries for higher performance. Once features are transformed, Workers batch samples together into materialized tensors, which are ready to be loaded onto GPU trainers. We ensure that transient delays in the pipeline do not introduce data stalls by maintaining a small buffer of tensors in memory.

4.1.3 Trainers. DPP Clients form the other half of the data plane. A Client runs on each training node, exposing a hook that the PyTorch runtime can call to obtain preprocessed tensors. These requests are transparently transformed into a simple *getData(numBatches)* API call, which returns *numBatches* of materialized tensors from the Worker buffer. By offloading computationally expensive operations to DPP Workers and enabling Client multithreading, Clients do not bottleneck the data ingestion pipeline. To ensure that Client and Worker network connections can scale, each Client uses partitioned round robin routing, capping the number of connections that Clients and Workers need to maintain.

To enable training larger recommendation models, we have built high-performance training clusters, enabling individual jobs to train on up to 16 servers, each with 8 GPUs. Each training job is controlled by a Trainer Master, which manages the overall training session as we describe in Section 5. On each trainer, a PyTorch runtime manages the local training workflow, transferring preprocessed tensors

| Model Class | # Float Features | # Sparse Features | # Derived Features |
|-------------|------------------|-------------------|--------------------|
| RM1 | 1221 | 298 | 304 |
| RM2 | 1113 | 306 | 317 |
| RM3 | 504 | 42 | 1 |

Table 5. Feature characteristics of production models.

| Dataset | # Float Feat. | # Sparse Feat. | Avg. Coverage | Avg. Len. | % Feat. Used | % Bytes Used |
|---------|------------------|-------------------|------------------|--------------|-----------------|-----------------|
| RM1 | 12115 | 1763 | 0.45 | 25.97 | 11 | 37 |
| RM2 | 12596 | 1817 | 0.41 | 25.57 | 10 | 34 |
| RM3 | 5707 | 188 | 0.29 | 19.64 | 9 | 21 |

Table 6. Dataset characteristics for each model. **Feat.** = Features

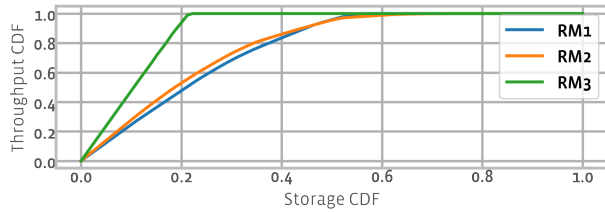


Figure 7. Reuse analysis, showing CDF of popular bytes to throughput absorbed, across one month of runs.

between the DPP Client and GPU device memory. Parameter updates between trainers occur over a dedicated backend network and do not impact data ingestion.

4.2 Co-designing Data Ingestion for Training

While our disaggregated architecture can meet data ingestion requirements, *we still required significant power and compute resources for data ingestion*. This hampered our training capacity as we had a fixed power budget. To address this, we co-designed storage and preprocessing for system efficiency with a deep understanding (§4.2.1) of our training workloads.

We primarily focused on improving the resource efficiency of DPP Workers and distributed storage nodes. By enabling *feature flattening* and *in-memory flatmaps* (§4.2.2), more resources can be used for expensive transformations, thus increasing the preprocessing throughput at each Worker. To improve storage efficiency, we observe that our HDD-based storage nodes are I/O bound, requiring us to size capacity for storage throughput. By optimizing for high-throughput reads via *merged reads* and *feature reordering* (§4.2.3), we reduced the amount of storage nodes required.

4.2.1 Understanding Training Data Properties. The aforementioned optimizations required leveraging characteristics of how training jobs ingest data. To understand this, we analyzed $RM_{1,2,3}$ to answer two primary questions: (a) "What fraction of training data do jobs use?", and (b) "Is there locality in commonly-used training data between multiple jobs?"

First, we looked at one instance of a production model for each RM . Recall that individual jobs specify a *feature projection*, containing a list of used features, while the Hive table itself may store more features than are used by an individual job. Table 5 shows the number of dense, sparse, and derived features required by each RM . These models require 504 – 1221 and 42 – 306 dense and sparse features, respectively. In contrast, Table 6 shows that significantly more features are logged in each model’s respective Hive tables. *Each training job only needs 9 – 11% of stored features*.

Individual features may vary in storage size due to coverage and list lengths. Features used in each model typically exhibit larger coverage and lengths, as they represent a stronger signal and are thus favored by ML engineers. Regardless, when we examine which bytes are read, Table 6 highlights that $RM_{1,2,3}$ only read 21 to 37% of stored bytes.

While there appears to be room to optimize for storage and reduce feature collection, feature experimentation is essential for ML engineers. Having a pool of features readily available to test in new model architectures is often worth the extra storage. However, we will co-design for the common case of jobs training only on a small subset of data.

We first need to examine if the small subset of data remains popular across multiple training jobs and over time. Figure 7 shows that training runs for $RM_{1,2,3}$ over a one month period tend to favor specific bytes. The x-axis shows a CDF of the model’s specified dataset. The y-axis shows the percent of all I/O from storage that the most-popular x percent of stored bytes contribute to. To serve 80% of traffic from storage, we only require the most popular 39, 37, and 18 percent of RM_1 , RM_2 , and RM_3 ’s dataset, respectively.

We will use the observations above to optimize DPP Workers and storage nodes.

4.2.2 DPP Worker Efficiency. We improved DPP Worker efficiency by optimizing how training data is stored in both data warehouse tables and Worker memory through *feature flattening* and *in-memory flatmaps*, respectively.

Feature Flattening. Feature flattening pushes data filtering to storage nodes, reducing Worker resources required to extract unnecessary bytes. Recall that features are stored in columnar format, with maps laid out in storage as two columns: one for keys and one for values. Figure 8 highlights how to access even a single feature, all keys and values for a given row must be read from storage. Since a large percent of features are filtered (see Table 6), this results in a large "over read" of bytes from storage.

Dedicating an individual column to each feature is not feasible. Table 6 shows that our datasets have thousands of features; new features are continually added and removed. With hundreds of models and tables, having a standard schema with limited feature columns across our training datasets is important for compatibility.

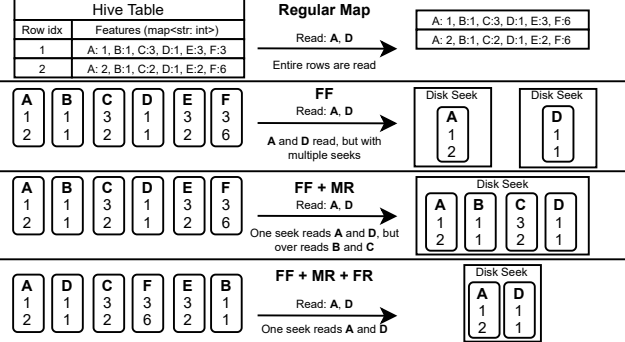


Figure 8. Example highlighting which features are read given regular map, FF=feature flattening, MR=merged reads, and FR=feature reordering.

| Experiment | Normalized Reader Throughput | % CPU Cycles on Extraction |
|--------------------|------------------------------|----------------------------|
| Baseline | 1.00 | 63 |
| Feature Flattening | 2.00 | 42 |

Table 7. Throughput and CPU cycles spent on extract operations for feature flattening on RM_1 's dataset.

Instead of changing the table schema itself, *feature flattening* breaks regular maps into flat map structures. It organizes maps so that values for a given feature ID, across rows, are stored contiguously on disk. Figure 8 compares feature flattening with regular maps. Given a feature projection (i.e., a list of used features), DPP can selectively read only the relevant streams of data containing required features from disks. Table 7 shows how feature flattening doubles worker throughput for RM_1 , halving the number of required DPP Workers for a given training job. As significantly less compute was spent on data extraction (e.g., decoding, decrypting, and reconstructing rows from warehouse) for unused bytes, more compute could be dedicated to transformations.

In-Memory Flatmap. While feature flattening optimizes data formats on disk, in-memory flatmaps optimize how rows are represented in DPP Worker memory. Data extraction reconstructs the original rows, with features grouped in a map. During preprocessing, these maps are subsequently indexed, and values are copied and transformed via feature-specific operations into tensors. This results in a series of costly format changes, requiring significant CPU cycles and memory bandwidth on the Workers. Typically, converting from rows to tensors (without feature-specific transformations) requires over 25% of CPU cycles on the Workers.

To address this inefficiency in format conversions, Workers use in-memory flatmaps to store each feature ID's values contiguously across rows. Because this format matches both how feature flattening stores samples on disk and how tensors are represented, it reduces necessary format conversions. It also allows Workers to quickly copy large blocks of data

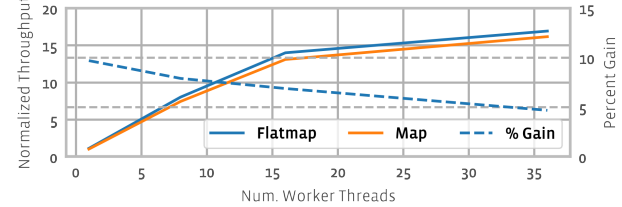


Figure 9. Worker throughput and percent improvement across number of Worker threads as in-memory flatmaps are applied.



Figure 10. Reduction in Storage Throughput and Payload Size overheads from storage due to feature reordering.

corresponding to a feature during transformations without needing to parse each row. Figure 9 shows the throughput at one DPP Worker as we increase the Worker thread count. Moving to in-memory flatmaps results in a 5 to 10% improvement in Worker throughput.

4.2.3 Storage IO Efficiency. The next two optimizations, *merged reads* and *feature reordering*, aim to increase the useful throughput from storage nodes. This is important as our training storage system is I/O bound and the number of required storage nodes is determined primarily based on throughput demands (as opposed to capacity).

Merged Reads. We currently use HDD-based storage nodes. HDDs are optimized for large reads by amortizing time for disk seeks. To increase the disk throughput and reduce the time spent on disk seeks, we read features that are placed close to one another in one ‘merged read’.

To illustrate the benefits, consider again the example in Figure 8. Assume each feature is 100KB in size, with features A and D placed non-contiguously in storage. Also assume a representative 12ms seek time and 200MB/s sequential read throughput. A merged read on the entire 400KB range between features A and D, including features B and C, is 1.79× faster than reading features A and D individually.

Feature Reordering. While merged reads increase storage throughput, it also over reads extra features squeezed between the necessary features, limiting its benefit. *Feature reordering* mitigates over reads by ordering popular features together.

Figure 10 shows that even after feature flattening and merged reads, there is still over a 100% over read of bytes from storage. This occurs because the offline preprocessing step that generates training data effectively orders feature

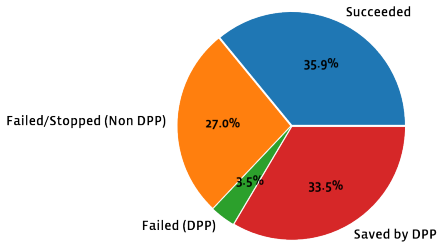


Figure 11. Breakdown of successful jobs, failed jobs (due to DPP and other factors), and jobs saved by DPP fault tolerance over a one week period.

columns randomly. In the example in Figure 8, reading features A and D with a merged read ends up over reading B and C, which are squeezed between A and D.

Feature reordering relies on co-designing our Warehouse write path based on the insight that a small set of popular features contribute to a large percent of storage throughput (Section 4.2.1). We analyzed a set of historic training jobs, across a one week window. Features that shared a similar hit rate (i.e., appeared in a similar fraction of training jobs) were reordered together on disk and written in new Hive tables used for future training runs. Combined with merged reads, this reduced the over read of bytes while better amortizing constant time disk seeks. Continuing the example in Figure 8, we can group A and D together into one merged read, thus minimizing over reads.

Figure 10 shows that a combination of feature flattening, merged reads, and feature reordering reduced both the amount of over read bytes and storage bandwidth overheads from over 100 percent to 8 and 20 percent, respectively. Since storage nodes are I/O bound, this allowed us to reduce storage power requirements by 1.94 \times .

4.3 Fault Tolerance

Fault tolerance is critical to prevent wasted compute and developer time, especially as jobs typically take days to complete. Figure 11 shows a breakdown of faults experienced in our GPU training jobs across a one week period. Only 35.9% jobs did not experience any fault, highlighting the importance of fault tolerance.

Fault tolerance is integrated across both DPP’s control and data planes. To enable checkpointing reader state, the DPP Master exposes two APIs to the Trainer Master: *createCheckpoint()* and *loadFromCheckpoint(state)*. These respectively allow the Trainer Master to create a checkpoint, obtaining a binary blob representing reader state (based on the remaining work items), and load reader state from that checkpoint. The DPP Master also continuously monitors worker health, automatically restarting any Workers that have failed without needing a checkpoint restore. The DPP Master itself is

replicated to avoid being a single point of failure. Finally, the DPP Master will obtain and hold a lease on the specific dataset during training to prevent modification.

DPP Workers’ stateless design directly enable fault tolerance, as they can simply re-fetch work items. Furthermore, Workers consistently report health information to the DPP Master, as well as important data and performance metrics to a centralized storage service. For ML engineers, DPP reports statistical distributions regarding each feature (e.g., popular categorical values, feature coverage, sparse feature lengths), which can be used to monitor for data quality alerts such as low feature coverage or feature drift. System metrics (e.g., buffer length, resource utilization, etc.) can monitor for bottlenecks in DPP and alert users of potential data stalls.

DPP Clients also play an important role during checkpointing. Once the Trainer Master issues a checkpoint request, the DPP Client ensures that all prefetch buffers are cleared before the checkpoint starts. Doing so prevents any loss of data during a checkpoint save or restore.

Through fault tolerance, DPP is able to automatically handle more than a majority of the faults shown in Figure 11. Only 3.5% of jobs needed to be recovered due to DPP failures. Digging deeper, we discovered that the majority of DPP failures occurred due to out-of-memory (32%) and filesystem (26%) errors, such as missing files. 27% of jobs failed or were stopped due to non-DPP related reasons; the majority of these jobs stopped due to user configuration error. Nevertheless, due to the checkpointing of DPP state, these jobs can quickly be resumed without loss of progress.

4.4 Effects of Disaggregation and Optimizations

By disaggregating storage and preprocessing, we ensure that large-scale training jobs do not stall waiting for data. For example, we were able to eliminate the 56% of GPU cycles stalled on data for RM_1 we described in Table 4, effectively doubling trainer throughput.

It is also critical to ensure that we drive down storage and preprocessing power costs. *At our scale, every efficiency gain is impactful*; a few percent improvement translates to megawatts of savings. We found multiple optimizations, such as removing unnecessary feature ID and null value checks, that allowed us to get 11% of throughput improvements on DPP Workers. We also leveraged build optimizations, including LTO (Linker Time Optimization) and AutoFDO [11], to obtain another 8% throughput improvement. Cumulatively, a set of localized optimizations resulted nearly 30% throughput improvement at each DPP Worker.

By leveraging how training jobs read data, as well as focusing on localized optimizations, we have been able to increase storage and reader throughput by 1.9 \times and 2.3 \times , respectively. This directly resulted in a 2.2 \times reduction in power required by the data ingestion pipeline, allowing us to provision more compute resources for training.

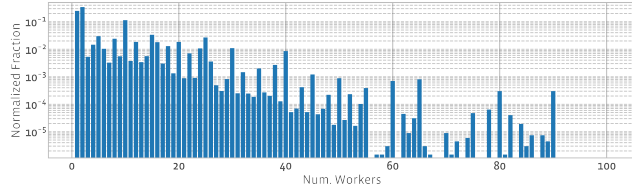


Figure 12. Normalized histogram of number of DPP workers used across jobs, within a two month period.

5 Deployment at Scale

DPP has been deployed for two years; we have onboarded the vast majority of our training workloads. It has enabled us to completely eliminate data stalls across our models.

Figure 12 shows a normalized histogram of the number of DPP workers requested across all training workloads over a two-month period. There are a large amount of small worker gangs, which represent the many small-scale experimental runs launched by ML engineers as a part of their feature engineering, model exploration, or hyperparameter tuning. With a simple configuration change, engineers can launch larger-scale training jobs, which represent a smaller fraction of the jobs, but require a large number of workers. Since each DPP worker is stateless and runs independently, DPP can achieve linear scaling to hundreds of workers for an individual job. In fact, the largest job required 256 DPP workers, which we do not show in Figure 12.

5.1 Frontend and Management

As shown in Figure 6, our data ingestion pipeline is integrated into our wider training ecosystem. ML engineers launch training jobs via FBLearn Flow [17], a centralized framework for training jobs. FBLearn Flow is designed to abstract away system management. It enables users to author complex training workflows, including the data ingestion pipeline, on top of hundreds of distributed nodes. Users simply provide a job configuration with the necessary information to configure, train, and evaluate a model.

For ease of use, the data ingestion configuration directly extends PyTorch’s current `DataSet` and `DataLoader` primitives [5]. Users populate a `HiveDataSet` with necessary specifications, including a) a *feature projection* listing all features used by the model, b) *transformations* for each feature, including those to derive new features, and c) a *dataset* corresponding to specific partitions within a Hive [46] table. Users also create a `DistributedDataLoader` on top of the `HiveDataSet`, which provides a simple iterator interface to obtain preprocessed tensors from DPP. Users configure the `DistributedDataLoader` to specify a degree of parallelism for DPP Workers. Currently, users rely on various services to determine how much DPP parallelism to dedicate to each job; predicting and right-sizing resources across ML models and use cases is a challenging task and beyond the scope of this

paper [14, 27]. Users leverage a set of libraries to generate the necessary configuration and launch jobs, all of which can be done from Python notebooks.

To start a job, our datacenter scheduler provisions the specified resources and launches the DPP Master, Workers, and Trainer nodes. It also launches a Trainer Master that manages the trainer nodes and coordinates control plane operations with the DPP Master. Nodes perform service discovery using a service similar to Zookeeper [22]. The Trainer Master sets up and starts the data ingestion pipeline by calling the `createSession()` API at the DPP Master. The Trainer Master also coordinates with the DPP Master to synchronize checkpoints. Both model and DPP checkpoints are published to a distributed blob store.

5.2 Capacity Planning

In addition to designing the data ingestion pipeline, we have to ensure that there are sufficient infrastructure resources to handle storage and bandwidth requirements. While we have multiple data centers (DC) in a region, cross-DC bandwidth is a constrained resource. At the same time, the large ingestion storage and bandwidth requirements of our training jobs preclude us from ignoring the cross-DC network.

We have built a sophisticated data placer and training job routing layer that makes training data storage and replication decisions based on the future demand of training pipelines. It tightly integrates with our cluster scheduler to intelligently route training jobs to GPU nodes that are in the same DC where the training data is stored. However, since DC power footprint is a fixed resource, we foresee the future need to shard data across DCs (or even geographic regions) due to dataset growth. We are actively working on methods to reconcile constrained network and storage requirements, such as leveraging checkpoints to cycle training jobs between DCs where the data is present.

Finally, we have dedicated considerable effort into accurately predicting and balancing storage, preprocessing, and training capacities within our fixed datacenter power budgets in order to achieve high resource utilization.

5.3 DPP Performance Testing Framework

To enable performance observability, we built a standalone performance testing framework that allows us to replay a training job’s data ingestion trace from its persistent DPP session information. By decoupling preprocessing from training via DPP, we can do so without requiring GPU trainers themselves. This has allowed us to integrate performance testing on actual models as a part of the testing and continuous integration framework across the data ingestion codebase. This ensures that even performance regressions of a few percent are detected, which can translate to megawatts of savings at our scale. Similarly, we validated the optimizations in Sections 4 and 6 via this framework.

| Server Type | Norm. Storage per Watt | Norm. Read BW per Watt |
|-------------|------------------------|------------------------|
| HDD | 1.00 | 1.00 |
| SSD | 0.09 | 3.26 |

Table 8. Normalized storage capacity and read bandwidth per watt for our HDD and SSD storage nodes.

6 Further Optimizations & Challenges

Caching and Tiered Storage: The reuse analysis in Figure 7 suggests that we can further optimize for popular feature placement and caching. We are exploring optimizations such as caching materialized tensors, which will reduce the amount of compute resources needed during preprocessing. We are also considering heterogeneous storage systems that combine HDDs and SSDs. Table 8 shows capabilities of the SSD and HDD storage nodes in our fleet. While HDDs provide a higher amount of storage per watt than SSDs, SSDs yield more read throughput per watt. Our current HDD-only storage system for training data is read I/O bound, while an SSD-only storage system would be bound by capacity and endurance challenges. An ideal solution would use each storage medium to its strength, balancing data between SSDs (for throughput) and HDDs (for capacity). For example, we could use a SSD-based cache for popular features.

Training Data Deduplication: We observe that ML engineers often build multiple training datasets from the same raw data source. For example, while RM_1 has one production dataset, there exist around 10 tables used for experimentation with slightly-different filtering and labeling configurations. Across our training datasets, each raw sample is represented around 5x across labeled datasets. Multiple datasets are used for developer efficiency and to reduce the amount of preprocessing operations necessary (e.g., filtering) during training, trading-off compute for increased storage. We are currently investigating ways to deduplicate our datasets efficiently by finding the right balance between storage and online preprocessing overheads.

Compute Optimizations: We are also investigating efforts to reduce the amount of compute at both DPP Workers and the trainer frontend. At DPP Clients, the largest compute overheads are caused by TLS decryption and memory management. For example, we are experimenting with more efficient authentication tokens, which has shown a 12 percent increase in DPP Client throughput. Longer term, we are investigating opportunities to accelerate “datacenter tax” operations [31, 45]. Note that the use of accelerators will not eliminate the need to right-size data preprocessing for each model using our disaggregated architecture. At DPP Workers, we considering improvements to how we store data. For example, pushing common operations such as sorting by feature ID to the offline ETL pipeline can reduce online preprocessing demands by 5 percent.

Optimizing the ML Training Pipeline End to End:

Compared to traditional content understanding (e.g., vision and NLP) models, recommendation models are significantly under-studied in the systems community relative to their importance in industry. This need for more focus is critical, as we estimate that the data ingestion power requirement for recommendation models is over 33x that required for content understanding workloads on our GPU training clusters. Unfortunately, many systems optimizations published for content understanding workloads (see Section 7), which optimize for unstructured collections of small files, are not applicable in our setting. They also do not address characteristics of how large ML models are trained in industry. While recommendation model benchmarks exist [33], they do not consider the data ingestion pipeline, nor are the datasets representative of our scale. We hope that this study can help the wider community to better understand, and optimize for, realistic industry-scale data ingestion pipelines.

7 Related Work

Data Ingestion for ML. tf.data [38] presents a runtime and API, inspired by LINQ [35], to construct a ML data ingestion pipeline for Tensorflow [7]. The tf.data runtime enables automatic optimizations to the preprocessing graph (e.g., operator fusion) and system parameters (e.g., prefetch buffer size, degree of request and thread parallelism). DPP similarly presents a runtime for data ingestion built on top of PyTorch [40]. Unlike tf.data that optimizes for preprocessing operations on the host CPU, DPP is inherently disaggregated. This enables preprocessing workers to scale to meet the throughput required by training jobs running on hundreds of GPUs. We also explore many orthogonal optimizations, such as warehouse data formats, that go beyond strictly preprocessing operations.

To motivate many of tf.data’s preprocessing optimizations, the authors performed a fleet-wide study of training jobs at Google. Our characterization results on recommendation models share many similar findings, such as the utility of data reuse and the large compute requirements of data ingestion. Our workloads also showed distinct differences that we optimize for, such as different storage formats, significantly larger dataset sizes, and complex preprocessing steps.

Other recent works target key components of the data ingestion pipeline, focusing on benchmark vision and NLP models. CoorDL [36] presents an in-memory caching algorithm to minimize disk I/O for single-server training. Quiver [29] implements a distributed cache on cloud VMs’ local SSD storage, optimizing for random ordering for hyperparameter tuning jobs. Similarly, DeepIO [52] and DLFS [53] leverage hardware support in the form of RDMA and NVMeOF to provide randomized minibatches from storage. DIESEL [47] co-designs storage and caching to provide efficient randomized minibatches for small files. Wang et al. [48] and Kumar

et al. [30] explore mitigating data stalls on TPUs. Finally, OneAccess [24] motivates how a shared data loading session can eliminate redundant work for hyperparameter tuning jobs. Our work differs as it focused on end-to-end characterization and optimization of data ingestion pipeline for large-scale recommendation model training that differ in several ways (large-scale distributed training, massive datasets, selective reading, and single-epoch training).

Recommendation Models. Recent work has explored the implications of large-scale recommendation systems across training and inference. Gupta et al. [20] analyzed industry-scale inference models on three different CPU architectures. DeepRecSys [19] optimized scheduling of inference requests across CPUs and GPUs. Acun et al. [8] characterized the implications of recommendation models’ architectures on GPU trainers.

Storage Formats for ML. Many storage formats for training data exist, such as Apache Avro [1], Apache Parquet [3], and TFRecord [6]. We store our datasets in Hive [46] tables in an Apache ORC [2] like format to enable a breadth of models and training jobs to share and experiment across a common dataset, as described in Section 3.1. The storage optimizations described in Section 4.2 leverage characteristics of how our recommendation models are trained at industry scale.

ETL Pipelines. Our data ingestion pipeline performs ETL operations, similar to Apache Spark [49], Beam [9], and other query engines. However, the PyTorch-based, per-minibatch preprocessing operations for recommendation models drastically differ from common queries performed on a relational database management system (RDBMS). Our data ingestion pipeline runs within a training job, optimizing for power-efficiency while avoiding data stalls, compared to query engines designed for high-throughput across multiple queries.

8 Conclusion

In this paper, we performed an end-to-end analysis and optimization of data ingestion pipelines for industry-scale recommendation models. We motivated and characterized the massive storage and preprocessing bandwidth required by distributed GPU trainers. To avoid the risk of starving trainers as models and accelerators become increasingly performant, we presented a fully disaggregated data ingestion pipeline. A important component is DPP, which allows preprocessing to scale out to meet the unique demands of each model’s training workload. We also highlighted the need for data ingestion system efficiency, especially as storage and preprocessing often requires more power than trainers themselves. We presented optimizations, co-designed across DPP, storage, and data warehouse, that reduced the power requirements of storage and preprocessing by 2.2×.

References

- [1] [n.d.]. Apache Avro. <https://avro.apache.org/>
- [2] [n.d.]. Apache ORC. <https://orc.apache.org/>
- [3] [n.d.]. Apache Parquet. <https://parquet.apache.org/>
- [4] [n.d.]. NVIDIA DGX Systems for Enterprise AI. <https://www.nvidia.com/en-us/data-center/dgx-systems/>
- [5] [n.d.]. PyTorch Datasets and Dataloaders. https://pytorch.org/tutorials/beginner/basics/data_tutorial.html
- [6] [n.d.]. TFRecord. https://www.tensorflow.org/tutorials/load_data/tfrecord
- [7] Martín Abadi, Paul Barham, Jianmin Chen, Zhifeng Chen, Andy Davis, Jeffrey Dean, Matthieu Devin, Sanjay Ghemawat, Geoffrey Irving, Michael Isard, Manjunath Kudlur, Josh Levenberg, Rajat Monga, Sherry Moore, Derek G. Murray, Benoit Steiner, Paul Tucker, Vijay Vasudevan, Pete Warden, Martin Wicke, Yuan Yu, and Xiaoqiang Zheng. 2016. TensorFlow: A System for Large-Scale Machine Learning. In *12th USENIX Symposium on Operating Systems Design and Implementation (OSDI 16)*. USENIX Association, Savannah, GA, 265–283. <https://www.usenix.org/conference/osdi16/technical-sessions/presentation/abadi>
- [8] Bilge Acun, Matthew Murphy, Xiaodong Wang, Jade Nie, Carole-Jean Wu, and Kim Hazelwood. 2020. Understanding Training Efficiency of Deep Learning Recommendation Models at Scale. *arXiv:2011.05497 [cs.AR]*
- [9] Tyler Akidau, Robert Bradshaw, Craig Chambers, Slava Chernyak, Rafael J. Fernández-Moctezuma, Reuven Lax, Sam McVeety, Daniel Mills, Frances Perry, Eric Schmidt, and Sam Whittle. 2015. The Dataflow Model: A Practical Approach to Balancing Correctness, Latency, and Cost in Massive-Scale, Unbounded, out-of-Order Data Processing. *Proc. VLDB Endow.* 8, 12 (Aug. 2015), 1792–1803. <https://doi.org/10.14778/2824032.2824076>
- [10] Luiz André Barroso, Urs Hözle, and Parthasarathy Ranganathan. 2018. The datacenter as a computer: Designing warehouse-scale machines. *Synthesis Lectures on Computer Architecture* 13, 3 (2018), i–189.
- [11] Dehao Chen, Tipp Moseley, and David Xinliang Li. 2016. AutoFDO: Automatic feedback-directed optimization for warehouse-scale applications. In *2016 IEEE/ACM International Symposium on Code Generation and Optimization (CGO)*. 12–23.
- [12] Heng-Tze Cheng, Levent Koc, Jeremiah Harmsen, Tal Shaked, Tushar Chandra, Hrishi Aradhye, Glen Anderson, Greg Corrado, Wei Chai, Mustafa Ispir, Rohan Anil, Zakaria Haque, Lichan Hong, Vihan Jain, Xiaobing Liu, and Hemal Shah. 2016. Wide & Deep Learning for Recommender Systems. In *Proceedings of the 1st Workshop on Deep Learning for Recommender Systems* (Boston, MA, USA) (DLRS 2016). Association for Computing Machinery, New York, NY, USA, 7–10. <https://doi.org/10.1145/2988450.2988454>
- [13] Jack Choquette and Wishwesh Gandhi. 2020. NVIDIA’s A100 GPU: Performance and Innovation for GPU Computing. In *2020 IEEE Hot Chips 32 Symposium (HCS), Virtual, August 16–18, 2020*. IEEE.
- [14] Eli Cortez, Anand Bonde, Alexandre Muzio, Mark Russinovich, Marcus Fontoura, and Ricardo Bianchini. 2017. Resource Central: Understanding and Predicting Workloads for Improved Resource Management in Large Cloud Platforms. In *Proceedings of the 26th Symposium on Operating Systems Principles (Shanghai, China) (SOSP ’17)*. Association for Computing Machinery, New York, NY, USA, 153–167. <https://doi.org/10.1145/3132747.3132772>
- [15] Paul Covington, Jay Adams, and Emre Sargin. 2016. Deep Neural Networks for YouTube Recommendations. In *Proceedings of the 10th ACM Conference on Recommender Systems* (Boston, Massachusetts, USA) (RecSys ’16). Association for Computing Machinery, New York, NY, USA, 191–198. <https://doi.org/10.1145/2959100.2959190>
- [16] Jeffrey Dean, Greg Corrado, Rajat Monga, Kai Chen, Matthieu Devin, Mark Mao, Marc’ aurelio Ranzato, Andrew Senior, Paul Tucker, Ke Yang, Quoc Le, and Andrew Ng. 2012. Large Scale Distributed Deep Networks. In *Advances in Neural Information Processing Systems*, F. Pereira, C. J. C. Burges, L. Bottou, and K. Q. Weinberger (Eds.), Vol. 25. Curran Associates, Inc. <https://proceedings.neurips.cc/paper/2012/file/6aca97005c68f1206823815f66102863-Paper.pdf>

[17] Jeffrey Dunn. 2018. Introducing FB Learner Flow: Facebook’s AI backbone. <https://engineering.fb.com/2016/05/09/core-data/introducing-fblearner-flow-facebook-s-ai-backbone/>

[18] Ali Mamdouh Elkahky, Yang Song, and Xiaodong He. 2015. A Multi-View Deep Learning Approach for Cross Domain User Modeling in Recommendation Systems. In *Proceedings of the 24th International Conference on World Wide Web (Florence, Italy) (WWW ’15)*. International World Wide Web Conferences Steering Committee, Republic and Canton of Geneva, CHE, 278–288. <https://doi.org/10.1145/2736277.2741667>

[19] U. Gupta, S. Hsia, V. Saraph, X. Wang, B. Reagan, G. Wei, H. S. Lee, D. Brooks, and C. Wu. 2020. DeepRecSys: A System for Optimizing End-To-End At-Scale Neural Recommendation Inference. In *2020 ACM/IEEE 47th Annual International Symposium on Computer Architecture (ISCA)*. 982–995. <https://doi.org/10.1109/ISCA45697.2020.00084>

[20] U. Gupta, C. Wu, X. Wang, M. Naumov, B. Reagan, D. Brooks, B. Cottel, K. Hazelwood, M. Hempstead, B. Jia, H. S. Lee, A. Malevich, D. Mudigere, M. Smelyanskiy, L. Xiong, and X. Zhang. 2020. The Architectural Implications of Facebook’s DNN-Based Personalized Recommendation. In *2020 IEEE International Symposium on High Performance Computer Architecture (HPCA)*. 488–501. <https://doi.org/10.1109/HPCA47549.2020.00047>

[21] K. Hazelwood, S. Bird, D. Brooks, S. Chintala, U. Diril, D. Dzhulgakov, M. Fawzy, B. Jia, Y. Jia, A. Kalro, J. Law, K. Lee, J. Lu, P. Noordhuis, M. Smelyanskiy, L. Xiong, and X. Wang. 2018. Applied Machine Learning at Facebook: A Datacenter Infrastructure Perspective. In *2018 IEEE International Symposium on High Performance Computer Architecture (HPCA)*. 620–629. <https://doi.org/10.1109/HPCA.2018.00059>

[22] Patrick Hunt, Mahadev Konar, Flavio P. Junqueira, and Benjamin Reed. 2010. ZooKeeper: Wait-free Coordination for Internet-scale Systems. In *2010 USENIX Annual Technical Conference (USENIX ATC 10)*. USENIX Association. <https://www.usenix.org/conference/usenix-atc-10/zookeeper-wait-free-coordination-internet-scale-systems>

[23] Norman P. Jouppi, Cliff Young, Nishant Patil, David Patterson, Gaurav Agrawal, Raminder Bajwa, Sarah Bates, Suresh Bhatia, Nan Boden, Al Borchers, Rick Boyle, Pierre-luc Cantin, Clifford Chao, Chris Clark, Jeremy Coriell, Mike Daley, Matt Dau, Jeffrey Dean, Ben Gelb, Tara Vazir Ghaemmehgami, Rajendra Gottipati, William Gulland, Robert Hagmann, C. Richard Ho, Doug Hogberg, John Hu, Robert Hundt, Dan Hurt, Julian Ibarz, Aaron Jaffey, Alek Jaworski, Alexander Kaplan, Harshit Khaitan, Daniel Killebrew, Andy Koch, Naveen Kumar, Steve Lacy, James Laudon, James Law, Diemthu Le, Chris Leary, Zhuyuan Liu, Kyle Lucke, Alan Lundin, Gordon MacKenan, Adriana Maggiore, Maire Mahony, Kieran Miller, Rahul Nagarajan, Ravi Narayanaswami, Ray Ni, Kathy Nix, Thomas Norrie, Mark Omernick, Narayana Penukonda, Andy Phelps, Jonathan Ross, Matt Ross, Amir Salek, Emad Samadiani, Chris Severn, Gregory Sizikov, Matthew Snelham, Jed Souter, Dan Steinberg, Andy Swing, Mercedes Tan, Gregory Thorson, Bo Tian, Horia Toma, Erick Tuttle, Vijay Vasudevan, Richard Walter, Walter Wang, Eric Wilcox, and Doe Hyun Yoon. 2017. In-Datacenter Performance Analysis of a Tensor Processing Unit. In *Proceedings of the 44th Annual International Symposium on Computer Architecture (Toronto, ON, Canada) (ISCA ’17)*. Association for Computing Machinery, New York, NY, USA, 1–12. <https://doi.org/10.1145/3079856.3080246>

[24] Aarati Kakaraparthi, Abhay Venkatesh, Amar Phanishayee, and Shivaram Venkataraman. 2019. The Case for Unifying Data Loading in Machine Learning Clusters. In *USENIX HotCloud*. <https://www.microsoft.com/en-us/research/publication/the-case-for-unifying-data-loading-in-machine-learning-clusters/>

[25] Svilen Kanev, Juan Pablo Darago, Kim Hazelwood, Parthasarathy Ranganathan, Tipp Moseley, Gu-Yeon Wei, and David Brooks. 2015. Profiling a Warehouse-Scale Computer. In *Proceedings of the 42nd Annual International Symposium on Computer Architecture* (Portland, Oregon) (*ISCA ’15*). Association for Computing Machinery, New York, NY, USA, 158–169. <https://doi.org/10.1145/2749469.2750392>

[26] Andrej Karpathy. 2018. Software 2.0. <https://medium.com/@karpathy/software-2-0-a64152b37c35>

[27] Ana Klimovic, Heiner Litz, and Christos Kozyrakis. 2018. Selecta: Heterogeneous Cloud Storage Configuration for Data Analytics. In *2018 USENIX Annual Technical Conference (USENIX ATC 18)*. USENIX Association, Boston, MA, 759–773. <https://www.usenix.org/conference/atc18/presentation/klimovic-selecta>

[28] Alex Krizhevsky. 2014. One weird trick for parallelizing convolutional neural networks. [arXiv:1404.5997 \[cs.NE\]](https://arxiv.org/abs/1404.5997)

[29] Abhishek Vijaya Kumar and Muthian Sivathanu. 2020. Quiver: An Informed Storage Cache for Deep Learning. In *18th USENIX Conference on File and Storage Technologies (FAST 20)*. USENIX Association, Santa Clara, CA, 283–296. <https://www.usenix.org/conference/fast20/presentation/kumar>

[30] Sameer Kumar, James Bradbury, Cliff Young, Yu Emma Wang, Anselm Levskaya, Blake Hechtman, Dehao Chen, HyoukJoong Lee, Mehmet Deveci, Naveen Kumar, Pankaj Kanwar, Shibo Wang, Skye Wanderman-Milne, Steve Lacy, Tao Wang, Tayo Oguntebi, Yazhou Zu, Yuanzhong Xu, and Andy Swing. 2021. Exploring the limits of Concurrency in ML Training on Google TPUs. [arXiv:2011.03641 \[cs.LG\]](https://arxiv.org/abs/2011.03641)

[31] Nikita Lazarev, Shaojie Xiang, Neil Adit, Zhiru Zhang, and Christina Delimitrou. 2021. *Dagger: Efficient and Fast RPCs in Cloud Microservices with near-Memory Reconfigurable NICs*. Association for Computing Machinery, New York, NY, USA, 36–51. <https://doi.org.stanford.edu.oclc.org/10.1145/3445814.3446696>

[32] Michael Lui, Yavuz Yetim, Özgür Özkan, Zhuoran Zhao, Shin-Yeh Tsai, Carole-Jean Wu, and Mark Hempstead. 2020. Understanding Capacity-Driven Scale-Out Neural Recommendation Inference. [arXiv:2011.02084 \[cs.DC\]](https://arxiv.org/abs/2011.02084)

[33] Peter Mattson, Christine Cheng, Gregory Diamos, Cody Coleman, Paulius Micikevicius, David Patterson, Hanlin Tang, Gu-Yeon Wei, Peter Bailis, Victor Bittorf, David Brooks, Dehao Chen, Debo Dutta, Udit Gupta, Kim Hazelwood, Andy Hock, Xinyuan Huang, Daniel Kang, David Kanter, Naveen Kumar, Jeffery Liao, Deepak Narayanan, Tayo Oguntebi, Gennady Pekhimenko, Lillian Pentecost, Vijay Janapa Reddi, Taylor Robie, Tom St John, Carole-Jean Wu, Lingjie Xu, Cliff Young, and Matei Zaharia. 2020. MLPerf Training Benchmark. In *Proceedings of Machine Learning and Systems*, I. Dhillon, D. Papailiopoulos, and V. Sze (Eds.), Vol. 2. 336–349. <https://proceedings.mlsys.org/paper/2020/file/02522a2b2726fb0a03bb19f2d8d9524d-Paper.pdf>

[34] Ivan Medvedev, Haotian Wu, and Taylor Gordon. 2019. Powered by AI: Instagram’s Explore recommender system. <https://ai.facebook.com/blog/powerd-by-ai-instagram-explore-recommender-system/>

[35] Erik Meijer, Brian Beckman, and Gavin Bierman. 2006. LINQ: Reconciling Object, Relations and XML in the .NET Framework. In *Proceedings of the 2006 ACM SIGMOD International Conference on Management of Data* (Chicago, IL, USA) (*SIGMOD ’06*). Association for Computing Machinery, New York, NY, USA, 706. <https://doi.org/10.1145/1142473.1142552>

[36] Jayashree Mohan, Amar Phanishayee, Ashish Raniwala, and Vijay Chidambaram. 2021. Analyzing and Mitigating Data Stalls in DNN Training. In *VLDB 2021*. <https://www.microsoft.com/en-us/research/publication/analyzing-and-mitigating-data-stalls-in-dnn-training/>

[37] Dheevatsa Mudigere, Yuchen Hao, Jianyu Huang, Andrew Tulloch, Srinivas Sridharan, Xing Liu, Mustafa Ozdal, Jade Nie, Jongsoo Park, Liang Luo, Jie Amy Yang, Leon Gao, Dmytro Ivchenko, Aarti Basant, Yuxi Hu, Jiyang Yang, Ehsan K. Ardestani, Xiaodong Wang, Rakesh Komuravelli, Ching-Hsiang Chu, Serhat Yilmaz, Huayu Li, Jiyuan Qian, Zhuobo Feng, Yinbin Ma, Junjie Yang, Ellie Wen, Hong Li, Lin Yang, Chonglin Sun, Whitney Zhao, Dimitry Melts, Krishna Dhulipala, KR Kishore, Tyler Graf, Assaf Eisenman, Kiran Kumar Matam, Adi Gangidi, Guoqiang Jerry Chen, Manoj Krishnan, Avinash Nayak,

Krishnakumar Nair, Bharath Muthiah, Mahmoud khorashadi, Pal-lab Bhattacharya, Petr Lapukhov, Maxim Naumov, Lin Qiao, Mikhail Smelyanskiy, Bill Jia, and Vijay Rao. 2021. High-performance, Distributed Training of Large-scale Deep Learning Recommendation Models. arXiv:2104.05158 [cs.DC]

[38] Derek G. Murray, Jiri Simsa, Ana Klimovic, and Ihor Indyk. 2021. tf.data: A Machine Learning Data Processing Framework. arXiv:2101.12127 [cs.LG]

[39] Satadru Pan, Theano Stavrinos, Yunqiao Zhang, Atul Sikaria, Pavel Zakharov, Abhinav Sharma, Shiva Shankar P, Mike Shuey, Richard Wareing, Monika Gangapuram, Guanglei Cao, Christian Preseau, Pratap Singh, Kestutis Patiejunas, JR Tipton, Ethan Katz-Bassett, and Wyatt Lloyd. 2021. Facebook’s Tectonic Filesystem: Efficiency from Exascale. In *19th USENIX Conference on File and Storage Technologies (FAST 21)*. USENIX Association, 217–231. <https://www.usenix.org/conference/fast21/presentation/pan>

[40] Adam Paszke, Sam Gross, Francisco Massa, Adam Lerer, James Bradbury, Gregory Chanan, Trevor Killeen, Zeming Lin, Natalia Gimelshein, Luca Antiga, Alban Desmaison, Andreas Kopf, Edward Yang, Zachary DeVito, Martin Raison, Alykhan Tejani, Sasank Chilamkurthy, Benoit Steiner, Lu Fang, Junjie Bai, and Soumith Chintala. 2019. PyTorch: An Imperative Style, High-Performance Deep Learning Library. In *Advances in Neural Information Processing Systems*, H. Wallach, H. Larochelle, A. Beygelzimer, F. d’Alché-Buc, E. Fox, and R. Garnett (Eds.), Vol. 32. Curran Associates, Inc. <https://proceedings.neurips.cc/paper/2019/file/bdbca288fee7f92f2bfa9f7012727740-Paper.pdf>

[41] Yves Raimond. 2018. Deep Learning for Recommender Systems. <https://www.slideshare.net/moustaki/deep-learning-for-recommender-systems-86752234>

[42] Alexander J. Ratner, Braden Hancock, and Christopher Ré. 2019. The Role of Massively Multi-Task and Weak Supervision in Software 2.0. In *CIDR 2019, 9th Biennial Conference on Innovative Data Systems Research, Asilomar, CA, USA, January 13-16, 2019, Online Proceedings*. www.cidrdb.org. <http://cidrdb.org/cidr2019/papers/p58-ratner-cidr19.pdf>

[43] I. S. Reed and G. Solomon. 1960. Polynomial Codes Over Certain Finite Fields. *J. Soc. Indust. Appl. Math.* 8, 2 (1960), 300–304. <https://doi.org/10.1137/0108018> arXiv:<https://doi.org/10.1137/0108018>

[44] Sebastian Ruder. 2017. An overview of gradient descent optimization algorithms. arXiv:1609.04747 [cs.LG]

[45] Akshitha Sriraman and Abhishek Dhanotia. 2020. Accelerometer: Understanding Acceleration Opportunities for Data Center Overheads at Hyperscale. In *Proceedings of the Twenty-Fifth International Conference on Architectural Support for Programming Languages and Operating Systems* (Lausanne, Switzerland) (ASPLOS ’20). Association for Computing Machinery, New York, NY, USA, 733–750. <https://doi.org/10.1145/3373376.3378450>

[46] Ashish Thusoo, Joydeep Sen Sarma, Namit Jain, Zheng Shao, Prasad Chakka, Suresh Anthony, Hao Liu, Pete Wyckoff, and Raghatham Murthy. 2009. Hive: A Warehousing Solution over a Map-Reduce Framework. *Proc. VLDB Endow.* 2, 2 (Aug. 2009), 1626–1629. <https://doi.org/10.14778/1687553.1687609>

[47] Lipeng Wang, Songgao Ye, Baichen Yang, Youyou Lu, Hequan Zhang, Shengen Yan, and Qiong Luo. 2020. DIESEL: A Dataset-Based Distributed Storage and Caching System for Large-Scale Deep Learning Training. In *49th International Conference on Parallel Processing - ICPP* (Edmonton, AB, Canada) (ICPP ’20). Association for Computing Machinery, New York, NY, USA, Article 20, 11 pages. <https://doi.org/10.1145/3404397.3404472>

[48] Yu Wang, Gu-Yeon Wei, and David Brooks. 2020. A Systematic Methodology for Analysis of Deep Learning Hardware and Software Platforms. In *Proceedings of Machine Learning and Systems*, I. Dhillon, D. Papailiopoulos, and V. Sze (Eds.), Vol. 2. 30–43. <https://proceedings.mlsys.org/paper/2020/file/c20ad4d76fe97759aa27a0c99bff6710-Paper.pdf>

[49] Matei Zaharia, Mosharaf Chowdhury, Tathagata Das, Ankur Dave, Justin Ma, Murphy McCauly, Michael J. Franklin, Scott Shenker, and Ion Stoica. 2012. Resilient Distributed Datasets: A Fault-Tolerant Abstraction for In-Memory Cluster Computing. In *9th USENIX Symposium on Networked Systems Design and Implementation (NSDI 12)*. USENIX Association, San Jose, CA, 15–28. <https://www.usenix.org/conference/nsdi12/technical-sessions/presentation/zaharia>

[50] Weijie Zhao, Deping Xie, Ronglai Jia, Yulei Qian, Ruiquan Ding, Mingming Sun, and Ping Li. 2020. Distributed Hierarchical GPU Parameter Server for Massive Scale Deep Learning Ads Systems. arXiv:2003.05622 [cs.DC]

[51] Guorui Zhou, Xiaoqiang Zhu, Chenru Song, Ying Fan, Han Zhu, Xiao Ma, Yanghui Yan, Junqi Jin, Han Li, and Kun Gai. 2018. Deep Interest Network for Click-Through Rate Prediction. In *Proceedings of the 24th ACM SIGKDD International Conference on Knowledge Discovery & Data Mining* (London, United Kingdom) (KDD ’18). Association for Computing Machinery, New York, NY, USA, 1059–1068. <https://doi.org/10.1145/3219819.3219823>

[52] Y. Zhu, F. Chowdhury, H. Fu, A. Moody, K. Mohror, K. Sato, and W. Yu. 2018. Entropy-Aware I/O Pipelining for Large-Scale Deep Learning on HPC Systems. In *2018 IEEE 26th International Symposium on Modeling, Analysis, and Simulation of Computer and Telecommunication Systems (MASCOTS)*. 145–156. <https://doi.org/10.1109/MASCOTS.2018.00023>

[53] Y. Zhu, W. Yu, B. Jiao, K. Mohror, A. Moody, and F. Chowdhury. 2019. Efficient User-Level Storage Disaggregation for Deep Learning. In *2019 IEEE International Conference on Cluster Computing (CLUSTER)*. 1–12. <https://doi.org/10.1109/CLUSTER.2019.8891023>